Optimized vector for functional expression of the human bitter taste receptor TAS2R14 in HEK293 cells

Christine Belloir, Adèle Gautier, Adeline Karolkowski, Thomas Delompré,
Mathilde Jeannin, Lucie Moitrier, Fabrice Neiers, Loïc Briand

Research Article

Optimized vector for functional expression of the human bitter taste receptor TAS2R14 in HEK293 cells

Christine Belloir, Adèle Gautier, Adeline Karolkowski, Thomas Delompré, Mathilde Jeannin, Lucie Moitrier, Fabrice Neiers, Loïc Briand [*]

Centre des Sciences Du Goût et de l'Alimentation, CNRS, INRAE, Institut Agro, Université de Bourgogne, F-21000, France

ABSTRACT

Bitter is one of the five basic taste qualities, along with salty, sour, sweet and umami, used by mammals to access the quality of their food and orient their eating behaviour. Bitter taste detection prevents the ingestion of food potentially contaminated by bitter-tasting toxins. Bitter taste perception is mediated by a family of G protein-coupled receptors (GPCRs) called TAS2Rs. Humans possess 25 TAS2Rs (human type II taste receptors), enabling the detection of thousands of chemically diverse bitter compounds. The identification of agonists/antagonists and molecular mechanisms that govern receptor-ligand interaction has been primarily achieved through functional expression of TAS2Rs in heterologous cells. However, TAS2R receptors, like many other GPCRs, suffer from marginal cell surface expression. In this study, we compared the functionality of 9 engineered chimeric receptors, focusing our experiments on TAS2R14, a broadly tuned receptor that recognizes over 151 identified compounds. Among the different tested signal peptides, rat somatostatin receptor subtype 3 results in higher potency of aristolochic acid-induced calcium signalling than other tested export tags, such as bovine rhodopsin, murine Igκ-chain or human mGluR5. The addition of a MAX sequence enhances both TAS2R14 potency and efficacy. We also confirm that the FLAG epitope, when located at the C-terminal, interferes less with the TAS2R14 functionality, enabling reliable evaluation of this receptor at the cell surface using immunohistochemistry. Finally, these observations are also confirmed for TAS2R14 and TAS1R2/TAS1R3 (the sweet taste receptor) stimulated by 12 bitter compounds and by sucralose and neotame, respectively.

1. Introduction

The sense of taste enables us to identify and discriminate key nutritional components present in food. Humans are able to discriminate five basic taste qualities, that are sweet, umami, bitter, salty and sour [1]. The bitter taste is thought to detect toxins, although an association between bitterness and toxicity is not always the case [2]. To detect gustatory stimuli, mammals have specialized taste receptor cells, which are organized into groups of 50–150 cells, forming a taste bud. One or multiple taste buds are mainly embedded within morphologically different taste papillae present on the surface of the tongue [3].

In humans, bitterness is detected through 25 G protein-coupled receptors (GPCRs) called TAS2Rs (type II taste receptor) [4–7]. Functional expression assays demonstrated that some TAS2Rs are tuned to detect a small array of structurally related compounds, whereas others are

sensitive to a large variety of chemically diverse bitter compounds [4,8]. This finding may explain how humans are able to detect thousands of bitter compounds with only 25 TAS2Rs. This recognition capacity was further expanded by the existence of a single nucleotide polymorphism on specific receptors exhibiting true phenotype activity [9–13]. TAS2R14, the most broadly tuned bitter taste receptor, is able to detect more than 151 identified bitter compounds perceived by humans with micromolar-range potency [14]. This receptor is widely characterized and activated by potent, structurally different bitter substances from both natural or synthetic origins [8,15–18]. Recently, cryo-electron microscopy structures of TAS2R14 complexed with G proteins were reported allowing identification of an orthosteric binding pocket occupied by cholesterol molecule as well as intracellular allosteric binding site [19–21].

Extra-oral expression of TAS2Rs widened the scope of action of bitter

---

compound-receptor interactions in other biological functions or patho-physiological states, such as disease and cancer [22–25]. TAS2R expression has been found in many extra-oral tissues and organs, including the gastro-intestinal tract [26–31], respiratory system [32–39], heart [40], genito-urinary system [41–43], breast [44], bone marrow and vascular system [45], skin [46,47], brain [48–51] and endocrine system [52]. For example, TAS2R14, is expressed in several extra-oral tissues and suggested to have physiological roles related to innate immune responses, male fertility and cancer [53]. These findings enhance TAS2R potential as a target for new emerging drugs.

Agonist and antagonist characterization have been mostly achieved using the functional expression of TAS2Rs in heterologous cell lines. However, a major drawback to investigating ligand-TAS2R relationships in mammals is their weak cell surface expression. To improve functional expression, TAS2Rs have been expressed as chimeric receptors containing the amino termini of either bovine rhodopsin (Rho) [5] or rat somatostatin receptor subtype 3 (SST3) [54].

The aim of this article was to identify TAS2R14 chimera that exhibited higher functional expression than widely approved gene construct used as a control (C). Our study was focused on TAS2R14 as broadly tuned receptor able to detect many bitter taste compounds. First, cellular assay was carried out using HEK293T stably expressing Gα16gut44 and transiently transfected with nine different human TAS2R14 (hTAS2R14) chimera constructs (including the construct C). Constructs varied according to the presence or absence of QBI SP163 translational amplifier sequence (MAX sequence), the tag epitope (FLAG) position and the signal peptide sequence (SST3, Rho, murine Igκ-chain (Igκ) and human mGluR5 (mGluR5)) that are favourably involved in functional expression. The activity of the nine TAS2R14 receptors stimulated by aristolochic acid was determined using calcium imaging experiments. Moreover, the validation of the enhancing response of the identified optimized vector was carried out with other known TAS2R14 agonists. Second, the protein expression and subcellular localization of the receptor were also analysed using immunocytochemistry and confocal microscopy. Third, the vector construction identified as exhibiting the best TAS2R14 activation was extended to other taste receptors, and in particular the sweet taste receptor TAS1R2/TAS1R3.

2. Materials and methods

2.1. Chemicals

The bitter molecules (aristolochic acid, picrotoxinin, 1-naphtoic acid, piperonylic acid, flufenamic acid, mefenamic acid, niflumic acid, diclofenac, tributyrin, santonin, genistein, (−)-α-thujone and parthenolide) were purchased from Sigma-Aldrich-Merck (Saint-Quentin Fallavier, France). Bitter compounds were freshly prepared and dissolved in buffer C1 (130 mM NaCl, 5 mM KCl, 10 mM HEPES, 2 mM CaCl₂, 10 mM pyruvic acid, pH 7.4, 300 mOsm) when they were soluble or in dimethyl sulfoxide (DMSO) at 100 mM for the initial solution of insoluble substance. After dilution in buffer C1 of the ranges of concentrations of ligand, DMSO never exceeded 0.1 % (v/v) to prevent toxic effects on cells. Dulbecco's modified Eagle's medium (DMEM) and all tissue culture media components were purchased from Life Technologies (St Aubin, France). The anti-FLAG M2 antibody was obtained from Sigma-Aldrich-Merck, and the Alexa 488-conjugated goat anti-mouse secondary antibody was obtained from Life Technologies.

2.2. Generation of TAS2R14 expression constructs

The chimeric Gα16gust44 was previously described [55]. This chimera was generated by replacing the C-terminal of Gα 16 with the C-terminal 44 residues of gustducin and cloned into the pcDNA3.1/-Hygro vector (Invitrogen, Thermo Fisher Scientific, Illkirch, France). The vector pcDNA5FRT-SST3-hTAS2R14-HSV, called vector control (C), was generously provided by Pr. W. Meyerhof (German Institute of

Human Nutrition Potsdam-Rehbruecke, Nuthetal, Germany). In the vector C, the full coding sequence of wild-type human TAS2R14 (NCBI accession number NM_023922) was amplified by PCR from human genomic DNA and cloned into the pcDNA5FRT vector from Invitrogen. The N-terminal contains the first 45 amino acids of rat somatostatin receptor subtype 3 (SST3) and a C-terminal sequence coding for a herpes simplex virus glycoprotein D epitope (HSV-tag) [16,54]. For the constructs used in this study, the 317 amino acid sequence of TAS2R14 was obtained from the online UniProt protein database (UniProt Q9NV8 also corresponding to NCBI accession number NM_023922.1). The coding region of TAS2R14 was cloned into the vector pcDNA4/myc-HisA (Invitrogen) between EcoRI and NotI restriction sites. This vector, named construct 1, constituted our internal laboratory control. Then, to improve protein expression in mammalian cells, we used human codon optimization (Genewiz, Leipzig, Germany). We tested, upstream of the start codon, a sequence called MAX, corresponding to the QBI SP163 element also described in pcDNA4-HisMax (Invitrogen). The QBI SP163 element is built together with a 31 nucleotide fragment of the 5′ cap sequence of the mouse vascular endothelial growth factor (VEGF) gene fused to a 132-nucleotide fragment of the 5′ untranslated region (UTR) immediately preceding the translational start site of the VEGF gene [56]. This final 163 nucleotide splice variant operates as a strong translational enhancer. To improve TAS2R14 functional expression, we explored two different signal peptides known to improve targeting of some GPCRs to the plasma membrane, including SST3 [57] and Rho [58]. We fused the first 45 amino acids of SST3 (MAAVTYPSSVPTTLDPGNAS-SAWPLDTSLGNASAGTSLAGLAVSG) or the 36 amino acids of Rho (MNGTEGPNFYVPFSNKTGVVRSPFEA PQYYLAEPWQ) in the N-terminal section of the gene. We also explored two other peptide signal sequences. The murine Igκ-chain leader sequence (Igκ) (METDTLLLWVLLLWVPGSTG) taken from the pSecTag2 vector (Invitrogen) is described for increasing protein secretion. The peptide signal sequence of human mGluR5 (MVLLLILSVLLLKEDVRGSA) leads to good expression of class C GPCR for CaSR [59] and GPRC6A [60]. Furthermore, we examined the impact of the FLAG sequence (DYKDDDDK) position between the N- or C-terminal on TAS2R14 functional activity [61]. The FLAG epitope allows immunocytochemical detection of receptor expression, as well as the HSV-tag (QPELAPEDPEDC). We constructed 8 vectors sharing different sequences described in Fig. 1. All plasmids were amplified with the QIAfilter Plasmid Midi kit (Qiagen, Courtabœuf, France). The final constructs were checked by DNA sequencing (Genewiz) for further use in all subsequent cellular studies.

2.3. Generation of TAS1R2 and TAS1R3 expression constructs

Initial TAS1R2 and TAS1R3 constructs were previously described [55]. TAS1R2 and TAS1R3 were amplified from human genomic DNA and assembled using overlapping primers. The open reading frames of TAS1R2 were cloned into pcDNA3, whereas TAS1R3 was inserted into pcDNA4-myc-HisA (Life Technologies), generating pcDNA3-TAS1R2 and pcDNA4-TAS1R3 plasmids. Then, two new vectors were engineered, and the coding region with native peptide signal of TAS1R2 (UniProt Q8TE23) and TAS1R3 (UniProt Q7RTX0) were cloned in pcDNA6-myc-HisA between HindIII and NotI and in pcDNA4-myc-HisA between EcoRI and NotI restriction sites, respectively. Codon optimization was used for human expression (Genewiz). Finally, upstream of the receptor coding sequence, the QBI SP163 translational element was added as described for TAS2R14 vectors, leading to pcDNA6-MAX-TAS1R2 and pcDNA4-MAX-TAS1R3 plasmids.

2.4. Calcium mobilization assay

HEK293T cells stably transfected with Gα16gut44 [55,62] were seeded on poly-D-lysine-coated 96-well black plates with a clear bottom (0.35x10⁵ cells/well) in high-glucose DMEM supplemented with 2 mM GlutaMAX, 10 % dialyzed foetal bovine serum Penicillin/Streptomycin
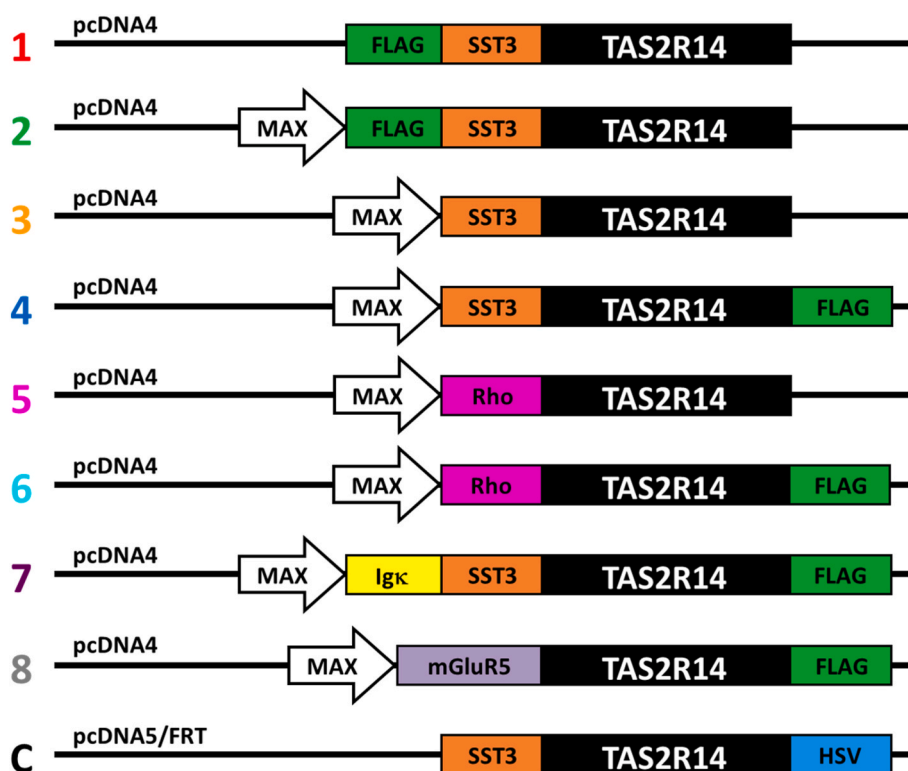
Fig. 1. Constructs used for the functional expression of human TAS2R14. Sequences were cloned in the pcDNA4 vector for constructs 1 to 8 and in pcDNA5/FRT for the vector C (control). The MAX enhancing translation sequence was inserted upstream for vectors 2 to 8. The signal peptide sequences were from rat somatostatin receptor subtype 3 (SST3), bovine rhodopsin (Rho), murine Igκ-chain leader (Igκ) and human mGluR5 (mGluR5). Epitope tags were added either in the N-terminal or C-terminal position, FLAG or Herpes simplex virus (HSV). The amino acid sequences of these 9 TAS2R14 constructs are detailed in Supplemental Table S1.

and G418 (400 μg/mL) at 37 °C and 6.3 % CO_2 in a humidified atmosphere. After overnight growth, cells were transiently transfected with TAS2R14 receptor constructs (120 ng/well) using Lipofectamine 2000 (0.4 μL/well) (Invitrogen), and experiments were conducted for all constructs the same day to ensure subsequent comparison of the data. For functional assay with the sweet taste receptor, cells were transiently transfected with TAS1R2 and TAS1R3 constructs (60 ng of each/well). We used FlexStation 3 (Molecular Devices, San Jose, CA, USA) to measure dose-response curves for each TAS2R14 vector. After 24 h, cells were loaded 1 h at 37 °C with Fluo4-AM (Molecular Probes, Sigma-Aldrich-Merck) previously mixed with Pluronic F-127 (0.01 %) and diluted in buffer C2 (130 mM NaCl, 5 mM KCl, 2 mM $CaCl_2$ 10 mM pyruvate, 10 mM Hepes; pH 7.4) containing 2.5 mM probenecid (Life Technologies). The calcium signal was recorded at 510 nm after excitation at 488 nm for 90 s, while the range of ligand was injected simultaneously in eight wells after 20 s using a microplate reader FlexStation 3. All substance concentrations were measured in triplicate wells at least three times independently. As cell transfection and bitter compounds could interfere with cellular viability and calcium assays, all compounds were tested on mock-transfected cells for all applied substance concentrations. Calcium signal emission was normalized to background fluorescence. The response from each well was calculated based on the ratio between maximum variation in fluorescence after ligand addition compared to initial fluorescence before addition and expressed as $\Delta F/F0$. The fluorescence signals collected for replicate were averaged for the same substance concentration, and the fluorescence changes of corresponding mock-transfected cells were subtracted. The dose-response data were fitted using a four-parameter logistic equation [$f(x) = min + (max - min)/(1 + (x/EC_{50})^{nH})$]. The median effective concentrations (EC_{50} values) and maximal amplitude values of receptor activation were generated using SigmaPlot software (Systat Software, San Jose, CA, USA).

2.5. Immunocytochemical staining of HEK293T cells

HEK293T-Gα16gust44 cells were seeded on 4-well culture slides (0.2×10^6 cells/well) precoated with Corning Cell-Tak adhesive. When the cells reached ~80 % confluence, they were transiently transfected with 600 ng cDNA TAS2R14 construct using 2 μL of Lipofectamine 2000 according to the manufacturer's recommendations. Approximately 24 h post-transfection, the cells were subjected to immunocytochemical staining. Cells were rinsed twice with Hank's HEPES balanced salt solution and cooled on ice for 1 h to avoid endocytosis. For the colocalization of the receptors with the plasma membrane, cells were incubated for 1 h on ice with 20 μg/mL biotin-concanavalin A (Sigma-Aldrich-Merck) that bound to glycoproteins. Then, the cells were washed and permeabilized for 5 min in cold acetone-methanol (1:1). After two washes with phosphate-buffered saline (PBS), the cells were blocked with 5 % goat serum in PBS for 1 h at room temperature. Next, for the staining receptor, the cells were incubated for 1 h with the primary antibodies mouse anti-FLAG M2 (Sigma F1804, Sigma-Aldrich-Merck) or mouse anti-HSV (Novagen, Sigma-Aldrich-Merck) diluted at 1/400 and 1/10,000, respectively, in Dako Antibody diluent (Dako, Agilent, Santa Clara, CA, USA). Cells were then rinsed twice with PBS, and the plasma membrane was visualized with the streptavidin Alexa Fluor 568 conjugate (Invitrogen, S11226) diluted at 1/2,000 in Dako Antibody diluent. After washing with PBS again, Alexa Fluor 488 goat anti-mouse antibody (Invitrogen) diluted at 1/2,000 was applied 1 h at room temperature. Finally, the cells were rinsed with deionized water, and the plastic chamber was detached from the culture slides. Coverslip was fixed with Mounting Medium (Dako). Finally, the cells were analysed using a fluorescence microscope (Nikon TiE, Nikon, Champigny-sur-Marine, France) equipped with a LucaR EMCCD Camera (Andor Technology, Belfast, UK) for TAS2R14 expression and a two-photon confocal microscope (Nikon A1-MP) equipped with an ×60 objective lens

(DImaCell (Cellular Imaging Device) platform, University of Bourgogne Franche-Comté, Dijon, France) for plasma membrane receptor colocalization.

3. Results

3.1. Functional characterization of TAS2R14 recombinants

3.1.1. Characterization of the vector C pcDNA5/FRT-SST3-hTAS2R14-HSV

To investigate the functional expression of TAS2R14 according to the peptide signal sequence and epitope tag position, calcium imaging experiments were performed. The dose-response relationships obtained by stimulating receptor-transfected cells with different concentrations of the bitter agonist aristolochic acid demonstrate the difference in the responsiveness of chimeric receptors resulting from all constructs (Fig. 1). The EC_{50} value for aristolochic acid using the pcDNA5/FRT-SST3-hTAS2R14-HSV vector (vector C) was 2.10 ± 0.41 μM with a maximal amplitude of 0.29 ± 0.01 (Fig. 2 and Table 1). These data are in accordance with previously published EC_{50} values of 2.0 μM [63] or with a slight difference, that is, 0.49 ± 0.03 μM [17].

3.1.2. Functional activity enhancement by MAX sequence

The constructs sharing the same FLAG-SST3-hTAS2R14 sequence but differing in the presence of a non-coding MAX enhancer (constructs 1 and 2) were compared to the vector C pcDNA5/FRT-SST3-hTAS2R14-HSV. For each construct, EC_{50}, as well as the maximal signal amplitude, were measured (Table 1). All 3 constructions caused a major response to the selected agonist, demonstrating that pcDNA4 and the pcDNA5/FRT plasmid are suitable for the functional expression of TAS2R14 (Fig. 2A). In our study, the pcDNA5/FRT was used as a traditional vector for transient transfection in HEK293T-Gα16gus44 cell lines without the FRT site. In our assay, the aristolochic acid responsiveness was slightly shifted towards a higher concentration range for

Table 1
EC_{50} values and maximal amplitudes generated by the different TAS2R14 constructs in response to aristolochic acid stimulation.

TAS2R14 construct	Sequence	EC_{50} (μM)	x-fold	Maximal amplitude	(%)
1	pcDNA4-FLAG-SST3-hTAS2R14	1.34 ± 0.11	1.57	0.24 ± 0.01	83
2	pcDNA4-MAX-FLAG-SST3-hTAS2R14	1.16 ± 0.12	1.81	0.31 ± 0.01	107
3	pcDNA4-MAX-SST3-hTAS2R14	1.05 ± 0.14	2.00	0.34 ± 0.01	117
4	pcDNA4-MAX-SST3-hTAS2R14-FLAG	0.76 ± 0.08	2.76	0.34 ± 0.01	117
5	pcDNA4-MAX-Rho-hTAS2R14	2.07 ± 0.26	1.01	0.30 ± 0.01	103
6	pcDNA4-MAX-Rho-hTAS2R14-FLAG	1.66 ± 0.15	1.26	0.31 ± 0.01	107
7	pcDNA4-MAX-Igκ-SST3- hTAS2R14-FLAG	1.53 ± 0.19	1.37	0.32 ± 0.01	110
8	pcDNA4-MAX-mGluR5-hTAS2R14-FLAG	–	–	0.18 ± 7.07	62
C	pcDNA5/FRT-SST3-hTAS2R14-HSV	2.10 ± 0.41	1.00	0.29 ± 0.01	100

SST3: rat somatostatin receptor subtype 3; Rho: bovine rhodopsin; Igκ: murine Igκ-chain leader; mGluR5: human mGluR5; HSV: Herpes simplex virus; C: control vector.

pcDNA5/FRT compared to the pcDNA4 vector (Fig. 2A). The two constructs pcDNA4-FLAG-SST3-hTAS2R14 (construct 1) and pcDNA4-MAX-FLAG SST3-hTAS2R14 (construct 2) are more sensitive, exhibiting EC_{50} values for aristolochic acid of 1.34 ± 0.11 and 1.16 ± 0.11 μM, respectively. We found that the presence of the MAX sequence improved the efficacy by 29 %. These results confirm the enhancer potential of the MAX sequence. Next, the MAX sequence was kept for all of our other TAS2R14 constructs.
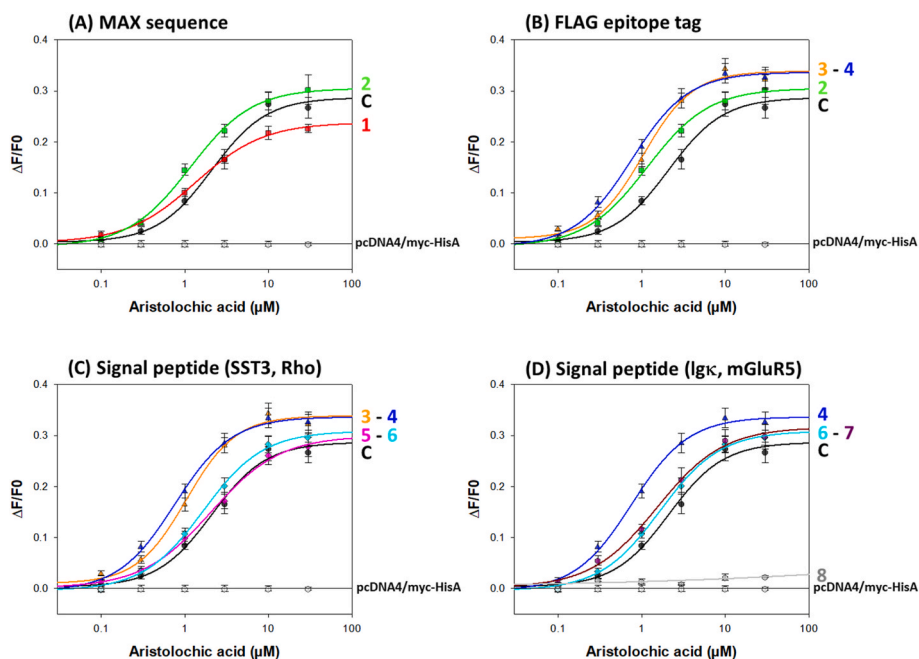

Fig. 2. Dose-response relationships of TAS2R14 constructs transfected in HEK293T-Gα16gus44 cells stimulated with aristolochic acid. Construct 1: pcDNA4-FLAG-SST3-hTAS2R14 (red); construct 2: pcDNA4-MAX-FLAG-SST3-hTAS2R14 (green); construct 3: pcDNA4-MAX-SST3-hTAS2R14 (orange); construct 4: pcDNA4-MAX-SST3-hTAS2R14-FLAG (blue); construct 5: pcDNA4-MAX-Rho-hTAS2R14 (pink); construct 6: pcDNA4-MAX-Rho-hTAS2R14-FLAG (turquoise); construct 7: pcDNA4-MAX-Igκ-SST3-hTAS2R14-FLAG (dark purple); construct 8: pcDNA4-MAX-mGluR5-hTAS2R14-FLAG (light grey); vector C (control): pcDNA5/FRT-SST3-hTAS2R14-HSV (black); empty vector: pcDNA4/myc-HisA (dark grey). Agonist was automatically applied to the transfected cells, and fluorescence changes were monitored. The logarithmically scaled x-axis indicates the aristolochic acid concentration (μM) and y-axis shows the relative changes of fluorescence upon agonist application. SST3: rat somatostatin receptor subtype 3; Rho: bovine rhodopsin; Igκ: murine Igκ-chain leader; mGluR5: human mGluR5; HSV: Herpes simplex virus.

3.1.3. Impact of FLAG tag and its position on functional activity

The FLAG epitope was inserted upstream or downstream of the SST3-hTAS2R14 sequence. Compared to the HSV-tag present in the construct 1, the FLAG-tag is commonly used to allow protein detection and purification when low levels of protein expression are expected [61,64,65]. None of the positions of the FLAG-tag prevented the transient expression of the gene of interest (Fig. 2B). Compared with the pcDNA4-MAX-SST3-hTAS2R14 construct without the tag sequence (construct 3), the aristolochic acid activation was the weakest when the FLAG sequence was inserted in the N-terminal position of the SST3-hTAS2R14 sequence (construct 2). Conversely, the functional expression of TAS2R14 was strongly enhanced when FLAG was omitted (construct 3) or placed in the C-terminal position (construct 4). Furthermore, the EC_{50} concentration was almost shifted to a 3-fold lower concentration, and the maximal amplitude increased by approximately 17 % for pcDNA-MAX-SST3-hTAS2R14-FLAG (construct 4) compared to the vector C (Table 1). A slight difference in aristolochic acid potency was observed between pcDNA4-MAX-SST3-hTAS2R14 (construct 3; 1.05 ± 0.14 μM) and pcDNA4-MAX-SST3-hTAS2R14-FLAG (construct 4; 0.76 ± 0.08 μM), and their efficacies were similar. Taken together, our results confirmed the modulation of TAS2R14 functional activity by the FLAG tag epitope. We also demonstrated that the C-terminal position was preferable and could slightly improve TAS2R14 sensitivity.

3.1.4. Influence of peptide signal sequence enhancing expression and/or membrane targeting

We compared the first 45 amino acids of the sequence SST3, which was also present in the vector C, with the 36 amino acids of Rho. The exchange of the signal peptide sequence SST3 (construct 3) to Rho (construct 5) in the pcDNA4-MAX-SST3-hTAS2R14 sequence led to a right shift of the dose-response curves (Fig. 2C). The EC_{50} value (2.07 ± 0.26 μM) and the signal amplitude (0.30 ± 0.01) of the construct 5 were similar to those of the vector C (Table 1). Note that the FLAG-tag in the C-terminal on the pcDNA4-Rho-hTAS2R14-FLAG (construct 6) resulted in a slightly larger effect on the calcium response compared to pcDNA4-Rho-hTAS2R14 (construct 5), as observed previously between the same construct with SST3 (constructs 3 and 4).

Therefore, we explored the response to aristolochic acid for the pcDNA4-MAX-Igκ-SST3-hTAS2R14-FLAG plasmid (construct 7). The addition of the Igκ chain leader sequence upstream of the SST3-hTAS2R14-FLAG sequence reduced responsiveness by 2-fold in potency to that measured for pcDNA4-MAX-SST3-hTAS2R14-FLAG (construct 4), leading to an equivalent response of pcDNA4-MAX-Rho-hTAS2R14-FLAG (construct 6) (Fig. 2D and Table 1). This result confirmed that the addition of the Igκ sequence to SST3 did not improve TAS2R14 functional expression more than SST3 alone.

Finally, we explored the exchange of the native TAS2R14 signal peptide sequence by the first 20 amino acids of the mGluR5 signal peptide. This leader sequence has been used to improve the functional expression of the CaSR receptor [59,60]. Surprisingly, TAS2R14 (construct 8) functional activity was abolished using this construct with a total loss of calcium signal response (Fig. 2D).

3.1.5. Validation of enhancing vector response with other TAS2R14 agonists

To validate the enhancing functional response of our best construct (pcDNA4-MAX-SST3-hTAS2R14-FLAG; construct 4), we tested twelve bitter compounds previously described for effective dose-response relationships with TAS2R14 [8,15–17]. We compared this construct with the control vectors in pcDNA5FRT (vector C) and in pcDNA4-FLAG-SST3-hTAS2R14 (construct 1). We studied different

agonists containing 3 ring structures with genistein, santonin, parthenolide and picrotoxinin; 2 rings for flufenamic acid and its derivates, mefenamic acid and diclofenac, niflumic acid, 1-naphtoic acid, piperonylic acid; 1 ring with (−)-α-thujone; and a linear structure with tributyrin (Fig. 3 and Table 2).

The EC_{50} values and maximal amplitudes for the vector C were similar to those of previous studies [8,15–17,66]. Functional expression of TAS2R14 showed a similar left shift of dose-response curves for pcDNA4-MAX-SST3-hTAS2R14-FLAG (construct 4) compared to the construct 1 and the vector C. The EC_{50} values were lower for pcDNA4-MAX-SST3-hTAS2R14-FLAG (construct 4) compared to the vector C stimulated by flufenamic acid, mefenamic acid, diclofenac and niflumic acid, indicating enhancement in potency. Surprisingly, the basal TAS2R14 construct in pcDNA4 without the MAX sequence (pcDNA4-FLAG-SST3-hTAS2R14, construct 1) led to EC_{50} values similar to pcDNA4-MAX (construct 4) for flufenamic acid and niflumic acid or even weaker for mefenamic acid, diclofenac and (−)-α-thujone. However, no significant difference in EC_{50} values was observed for these 3 vectors stimulated by genistein, parthenolide, picrotoxinin, 1-naphtoic acid and piperonylic acid. For all tested bitter agonists, with the exception of picrotoxinin and piperonylic acid, signal amplitude was strongly promoted by the enhancing transcriptional sequence (MAX sequence) and the presence of the FLAG epitope in the C-terminal position. Moreover, the difference in maximal amplitude was also enhanced by the MAX sequence compared to the vector C pcDNA5/FRT-SST3-hTAS2R14-HSV, although it was enhanced regarding genistein, parthenolide, 1-naphtoic acid and tributyrin. This short panel of tested ligands confirmed the enhancement of the functional response of the pcDNA4-MAX-SST3-hTAS2R14-FLAG construct (construct 4) for chemically diverse bitter compounds.

3.2. Cell surface expression

To assess the cell surface expression of TAS2R14 using the different constructs, we transiently and individually transfected each vector into HEK293T-Gα16gus44 cells. After immunocytochemical staining, we observed, in epifluorescence microscopy, significant TAS2R14 expression for all gene constructs without significant differences (Supplemental Fig. S1). Nevertheless, the staining of cells transfected by pcDNA4-MAX-mGluR5-hTAS2R14-FLAG (construct 8) showed accumulation of the receptor in the cytosol in the form of a fluorescent granule that suggests accumulation of the receptor within the Golgi compartment.

To validate cell plasma membrane surface expression and to investigate the reason for the decreased responsiveness of mGluR5-hTAS2R14-FLAG, we observed immunocytochemical colocalization, as analysed using confocal microscopy. As shown in Fig. 4, the merged image of immunofluorescence from the TAS2R14 receptor (green) and plasma membrane (red) shows colocalization for all FLAG-tagged constructs, except for the mGLuR5 signal peptide sequence (pcDNA4-MAX-mGluR5-hTAS2R14-FLAG; construct 8). These results agree with the absence of functional activity observed with pcDNA4-MAX-mGluR5-hTAS2R14 (construct 8), which can be attributed to the absence of membrane targeting.

3.3. Application of the optimized vector to sweet taste receptor TAS1R2/TAS1R3

To test whether the best construct obtained for TAS2R14 was transposable to other taste receptors, we designed new constructs for the two TAS1R2 and TAS1R3 subunits that composed the heterodimeric sweet taste receptor and investigated their functional activity using
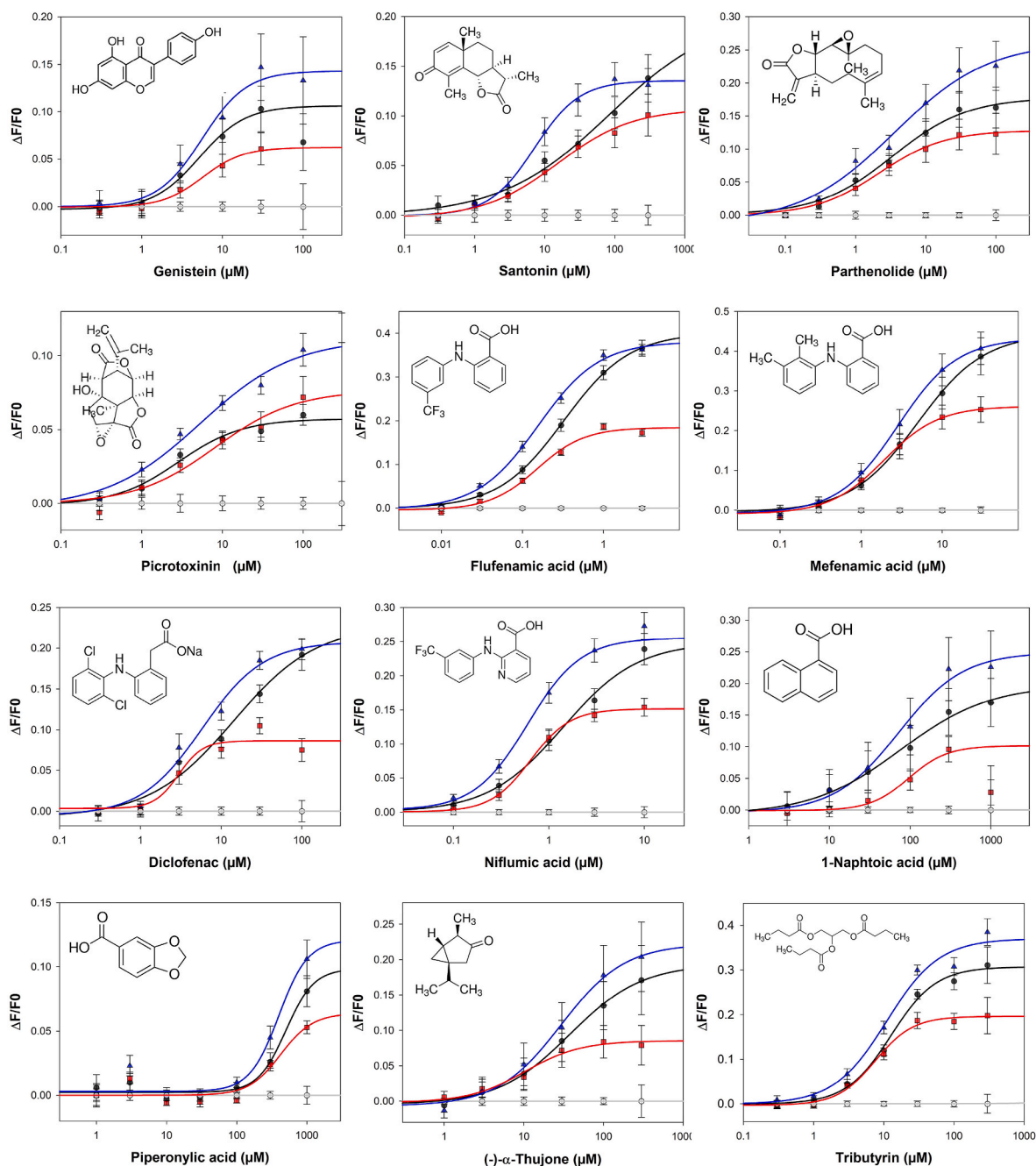
Fig. 3. Dose-response relationships of TAS2R14 constructs transfected in HEK293T-Gα16gus44 cells stimulated with various bitter compounds. HEK 293T-Gα16gust44 cells were transiently transfected with vector 4 pcDNA4-MAX-SST3-hTAS2R14-FLAG (blue), vector 1pcDNA-FLAG-SST3-hTAS2R14 (red) or vector C (control) pcDNA5/FRT-SST3-hTAS2R14-HSV (black) or empty vector pcDNA4/myc-HisA (grey). Agonist (presented with their chemical structure) was automatically applied to the transfected cells, and fluorescence changes were monitored. The logarithmically scaled x-axis indicates the compound concentration (μM) and y-axis shows the relative changes of fluorescence upon agonist application. SST3: rat somatostatin receptor subtype 3; HSV: Herpes simplex virus.

calcium-based cell assays with two sweeteners, sucralose and neotame. The dose-response relationships, the EC_{50} values and the maximal amplitude are presented in Fig. 5 and Table 3. The dose-response curves and the calculated EC_{50} and maximal amplitude values were similar to those of previous studies for pcDNA3-TAS1R2/pcDNA4-TAS1R3 [67–69]. The vector pcDNA3-MAX-TAS1R2/pcDNA4-MAX-TAS1R3 exhibited a lower EC_{50} value and higher maximal amplitude than pcDNA3-TAS1R2/pcDNA4-TAS1R3 and pcDNA3-MAX-TAS1R2/pcDN A4-TAS1R3 when stimulated by the sweeteners, sucralose and neotame. In addition, for neotame, the potency was higher for pcDNA3-TAS1R2/pcDNA4-MAX-TAS1R3 and pcDNA3-MAX-TAS1R2/pcDNA4-MAX-TAS1R3. Our results confirmed that the TAS1R

expression is also improved by this translational element (MAX sequence) as observed for TAS2R14.

4. Discussion

In the present study, we engineered an optimized construct for the functional expression of human TAS2R14 in HEK293 cells. To compare different constructs, we functionally expressed TAS2R14 with added or exchanged DNA sequences that are well known to achieve this goal in other GPCRs. Insertion of the MAX sequence upstream of gene synthesis strongly improved the potency and efficacy of the receptor without increasing the level of measurable expression at the cell surface. The QBI

Table 2

EC$_{50}$ values and maximal amplitudes generated by different TAS2R14 constructs in response to different bitter compounds.

TAS2R14 construct	1		4		C	
	pcDNA4-FLAG-SST3-hTAS2R14		pcDNA4-MAX-SST3-hTAS2R14-FLAG		pcDNA5/FRT-SST3-hTAS2R14-HSV	
	EC$_{50}$ (µM)	Maximal amplitude	EC$_{50}$ (µM)	Maximal amplitude	EC$_{50}$ (µM)	Maximal amplitude
Genistein	5.71 ± 1.77	0.06 ± 0.01	5.94 ± 1.37	0.14 ± 0.01	5.18 ± 0.61	0.11 ± 0.01
Santonin	15.53 ± 3.95	0.10 ± 0.01	7.14 ± 0.69	0.14 ± 0.01	85.03 ± 83.21	0.20 ± 0.05
Parthenolide	2.08 ± 0.33	0.13 ± 0.01	3.41 ± 1.19	0.25 ± 0.02	3.06 ± 0.65	0.17 ± 0.01
Picrotoxinin	8.22 ± 6.37	0.08 ± 0.02	5.32 ± 2.62	0.11 ± 0.02	2.84 ± 0.91	0.06 ± 0.01
Flufenamic acid	0.15 ± 0.03	0.18 ± 0.01	0.16 ± 0.02	0.38 ± 0.01	0.32 ± 0.01	0.40 ± 0.01
Mefenamic acid	1.92 ± 0.25	0.26 ± 0.01	2.85 ± 0.26	0.43 ± 0.01	5.01 ± 0.46	0.45 ± 0.02
Diclofenac	2.98 ± 0.81	0.09 ± 0.01	5.80 ± 1.65	0.21 ± 0.02	14.14 ± 8.95	0.23 ± 0.05
Niflumic acid	0.64 ± 0.04	0.15 ± 0.01	0.60 ± 0.12	0.26 ± 0.01	1.40 ± 0.29	0.25 ± 0.02
1-Naphtoic acid	95.95 ± 15.23	0.10 ± 0.01	77.20 ± 20.89	0.25 ± 0.02	76.27 ± 25.88	0.20 ± 0.02
Piperonylic acid	427 ± 170	0.05 ± 0.01	398 ± 274	0.12 ± 0.05	501 ± 480	0.10 ± 0.06
(−)-α-Thujone	0.29 ± 3.10	0.09 ± 0.01	29.35 ± 6.48	0.22 ± 0.02	37.85 ± 8.06	0.19 ± 0.02
Tributyrin	7.53 ± 0.95	0.20 ± 0.01	10.94 ± 2.58	0.37 ± 0.03	12.65 ± 1.56	0.31 ± 0.01

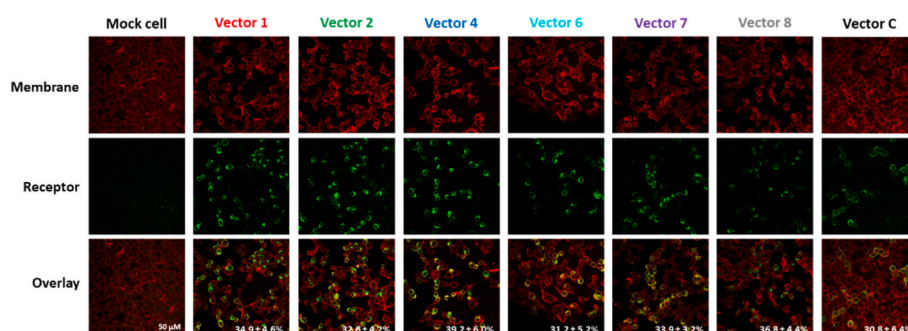SST3: rat somatostatin receptor subtype 3; HSV: Herpes simplex virus; C: vector control.

Fig. 4. Cell-surface localization and expression rates of TAS2R14 constructs. Immunocytochemistry of HEK293T-Gα16gust44 cells expressing various FLAG-tagged and HSV-tagged TAS2R14 constructs. The TAS2R-expressing cells are shown in green, and the plasma membrane is stained in red. The receptors were detected using a primary anti-FLAG or anti-HSV antibody and fluorescently labelled by a secondary Alexa-488–conjugated antibody. This experiment was not applied to vectors 3 and 5, which did not contain a FLAG tag in their construction. All data were obtained from the same transfection experiment. HEK293T-Gα16gust44 cells in the absence of the TAS2R14 receptor (mock cells) showed no signal. Pictures were taken using a two-photon confocal microscope (Nikon A1-MP) equipped with a 60x objective lens. The average cell fraction expressing the receptor (±SEM) is provided in white in the overlay panel. Four to six images were counted, and averaged per receptor construct pictures. The TAS2R14 constructs are presented in Fig. 1. HSV: Herpes simplex virus; C: vector control.
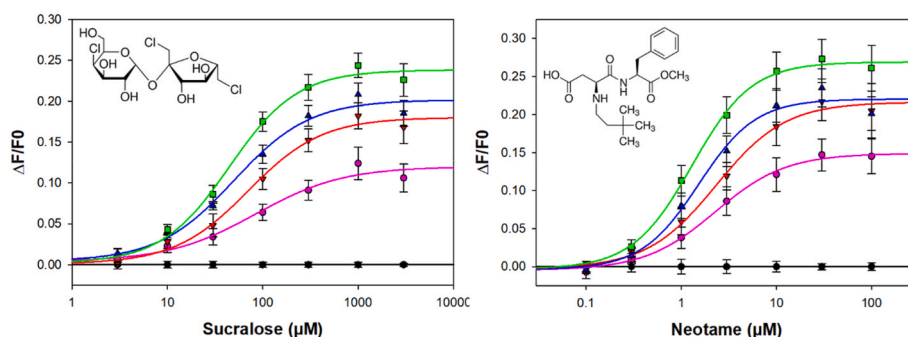

Fig. 5. Dose-response relationships of sweet taste receptor stimulated with sucralose and neotame using TAS1R2 and TAS1R3 expressing vectors promoted by QBI SP163 translational enhancer sequence (MAX sequence). HEK293T-Gα16gust44 cells were transiently co-transfected with vectors expressing each TAS1R2 and TAS1R3 subunit. Co-transfection of pcDNA3-TAS1R2 with pcDNA4-TAS1R3 (pink), or pcDNA3-MAX-TAS1R2 with pcDNA4-TAS1R3 (red), or pcDNA3-TAS1R2 with pcDNA4-MAX-TAS1R3 (blue) or pcDNA3-MAX-TAS1R2 with pcDNA4-MAX-TAS1R3 (green). Mocked cells did not respond to sweetener agonists (black). Agonists were automatically applied to the transfected cells, and fluorescence changes were monitored. The logarithmically scaled x-axis indicates the compound concentration (µM) and y-axis shows the relative changes of fluorescence upon agonist application.

SP163 translational element appeared to be a powerful tool to improve the functional expression of TAS2Rs. These elements can also be used for other GPCRs, as we demonstrated for the sweet taste receptor TAS1R2/TAS1R3.

We also observed that rat SST3, more than bovine Rho, favoured the functional expression of TAS2R14 in HEK293T-Gα16gust44 cells using calcium imaging experiments. Finally, we found that FLAG epitope tag addition in the C-terminal can also improve receptor functionality, enabling reliable evaluation of cell surface expression by immunocytochemistry.

This work showed that while the SST1 receptor was largely maintained in intracellular vesicles, the SST3 receptor was targeted to the cell

Table 3
EC$_{50}$ values and maximal amplitude generated by the TAS1R2 and TAS1R3 constructs in response to two sweeteners, sucralose and neotame.

TAS2R14 construct	Sucralose				Neotame			
	EC$_{50}$ (μM)	x-fold	Maximal amplitude	(%)	EC$_{50}$ (μM)	x-fold	Maximal amplitude	(%)
pcDNA3-TAS1R2/pcDNA4-TAS1R3	84.13 ± 32.75	1.00	0.12 ± 0.01	100	2.28 ± 0.29	1.00	0.15 ± 0.01	100
pcDNA3-MAX-TAS1R2/pcDNA4-TAS1R3	70.53 ± 13.43	1.19	0.18 ± 0.01	150	2.32 ± 0.32	0.98	0.22 ± 0.01	147
pcDNA3-TAS1R2/pcDNA4-MAX-TAS1R3	49.82 ± 11.12	1.69	0.20 ± 0.01	167	1.52 ± 0.28	1.50	0.22 ± 0.01	147
pcDNA3-MAX-TAS1R2/pcDNA4-MAX-TAS1R3	44.76 ± 6.15	1.88	0.24 ± 0.01	200	1.30 ± 0.13	1.75	0.27 ± 0.01	180

surface. Its N-terminal has been clearly demonstrated to be responsible for the main difference in subcellular destination. Analysis of receptor chimeras of SST1 and SST3 demonstrated that the first 65 amino acid residues of the N-terminal regions of SST3 are sufficient to obtain SST1 cell surface expression [57]. Then, these researchers used only the first 45 amino acids of the rat SST3 as a cell-surface-targeting signal at the N-terminal of bitter taste receptors [54] and started deorphanizing the 25 human TAS2Rs [8]. The SST3 receptor still serves as a mechanistic model for understanding endosomal trafficking of GPCR and intracellular signalling [70,71].

Other strategies have been used to enhance GPCR expression in heterologous systems [72]. Among these strategies, the insertion of the rhodopsin N-terminal 20 amino acid residues was widely used to improve cell surface targeting of functional olfactory receptors (ORs) in the same cellular model [58,73]. It was shown that the Rho-tag fusion fused to mouse ORs, as well as the FLAG-tag, generally leads to lower concentrations of agonist responses, thereby enhancing potency compared to HA-tagged or untagged ORs [73]. However, the authors showed that in cellular assays using OR transfection, increasing quantities of plasmid construction coding the OR during transfection contributes mainly to ligand specificity, suggesting that the quantity of cell-surface receptors, and not the Rho-tag, is involved in potency enhancement [73]. However, even with Rho-tag, many ORs still fail to reach the cell plasma membrane, and it was demonstrated that tags concatenation with the leucine-rich 17-amino acid signal peptide, such as Lucy-Rho-tag, in the N-terminal signal peptide could promote widespread OR surface expression [74]. More recently, it was demonstrated that replacement of the C-terminal domain of the difficult-to-express human OR5A2, by an altered-terminal spontaneous mutated sequence identified fortuitously, conferred to the OR5A2 the ability to be functionally expressed. The optimized sequence led to higher surface expression and improved sensitivity up to 15 times [75]. In another study, the optimization of the C-terminal amino acid sequence of OR7C1 led to higher cell surface expression and up to 500-fold improved sensitivity [76]. Concerning the bitter taste receptor, the first chimeric construct was obtained with the first 39 amino acids of bovine Rho, analogously to OR, and led to very effective targeting to the cell surface of human TAS2R4 [5]. The crystal structure resolution of Rho demonstrated that the first 36 amino acids correspond to the extracellular domain [77]. In the functional assay presented in this study, the Rho-tag sequence, inserted in pcDNA4-MAX, was as effective in enhancing the TAS2R14 response compared to the control vector pcDNA5/FRT-SST3-hTAS2R14-HSV, but the promoting effect with SST3 was more important in our own construct in pcDNA4-MAX.

We also used the FLAG-tag system to visualize TAS2R14 expression by immunostaining. FLAG-tag has become an extensively used tag system for identification, primarily for purification by a single-step procedure, of recombinant membrane proteins expressed in HEK cells [78]. Indeed, tags could overcome some difficulties in protein production by reducing aggregation, enhancing efficient translation, and increasing solubility. The small size, hydrophilic nature of sequence peptide, availability of high-affinity antibodies and ability to remove peptide via enterokinase cleavable sites make FLAG-tags essential biochemistry tools [61,79–81]. The only drawback of the FLAG-tag could be a post-translational modification due to the tyrosine sulfation in the motif DYK that abolishes the FLAG-anti-FLAG interaction [82]. In this study,

we demonstrated that the C-terminal FLAG-tag position interfered less with TAS2R14 functionality than the FLAG located in the N-terminal position. It seemed that the N-terminal FLAG-tag upstream position decreased the ligand binding affinity of TAS2R14 with aristolochic acid. This finding might be explained by a possible disturbance on the extracellular site, also known as the vestibular site, involved in the binding process and recently brought to light by a molecular dynamic approach with TAS2R46 bitter taste receptor [83] or OR [84]. Inversely, the C-terminal position of the FLAG-tag leads to a weak enhancement in potency, which could be explained by a favourable coupling with protein G. Indeed, a recent study highlighted the crucial role of the conserved KLK/R motif in the cytoplasmic C-terminal region of TAS2R4 [85]. Independent of the two highly conserved motifs in TM2 (LxxxR), inTM5 (LxxSL) or the 13 conserved residues shown to have critical roles in receptor activation [10,86], the author demonstrated by an alanine scan mutagenesis that the C-terminal KLK motif in TAS2R4 and, more precisely, the Lys300 of TAS2R4 is critical for receptor function and that basic and hydrophobic amino acid residues are important for trafficking and activation [85]. Compared to TAS2R4, TAS2R14 is composed of 35 amino acids in the C-terminal, and FLAG-tag added negatively charged residues, which could promote interaction with the G protein. The first full-length structure of the GPCR/G protein interface obtained for the β2-AR-G$_s$ complex demonstrated that 20 amino acids in the C-terminal of Gs are strongly involved in agonist affinity [87]. Thus far, the dynamic interaction mechanism between receptor and G protein subtype selectivity still requires more experiment to clearly understand coupling specificity. However, a study that tethered β2-AR and different Gαs terminal peptides demonstrated that even in the control sequence, the presence of the ER/K polylinker 1- alone at the C-terminal of the GPCR, 2- between the two protein domains, or 3- the use of scrambled peptide instead of Gs peptide or Gq peptide systematically increased receptor activity [88]. Thus, we hypothesized that the eight amino acids added by FLAG-tag in the C-terminal of TAS2R14 weakly contribute to enhancing its activity through structural stabilization of coupling active interactions between the receptor and endogenous G protein.

Other approaches have been investigated to improve TAS2R functionality, such as the role of accessory proteins serving as chaperones. Thus, the influence of the receptor transporting protein RTP and the receptor enhancing protein Reep have been evaluated [89]. Indeed, it has been previously shown that co-expression of RTP1, RTP2 and Reep1 can improve OR functionality [90], as well as the shorter form of RTP1 (RTP1S) [91,92] or the Myr-Ric-8A [93] and Ric-8B proteins [94,95]. Researchers have demonstrated that the introduction of RTP3 and RTP4 can influence cell surface trafficking and increase amounts of TAS2R16 receptor by 4- to 3-fold, respectively, leading to significant amplification of TAS2R-mediated signal transduction of the bitter taste receptor TAS2R16 [89]. Interestingly, RT-PCR analysis of HEK293T-Gα16gust44 revealed endogenous expression of RTP and REEP genes. Interestingly, heterologous expression of the sweet taste receptor TAS1R2/TAS1R3 and the bitter taste receptors TAS2R16 and TAS2R44 was enhanced by REEP2 due to the recruitment of the receptor to lipid raft microdomains [96].

Finally, the ability of the receptor to reach the cell surface may be affected by glycosylation. Similar to many cell surface proteins, TAS2R receptors are glycosylated on Asn. Sequence alignment of TAS2R has shown that the Asn-linked glycosylation residue in a conserved sequence

of ECL2 (extracellular loop 2) is conserved among all 25 hTAS2Rs. Mutation of this conserved sequence decreases receptor surface expression [97].

In conclusion, the aim of our work was to demonstrate the importance of the initial construction of GPCR to functionally express them in large amounts, targeting the cell surface and promoting the active state in a heterologous HEK293 cell line. Additionally, many other technical parameters, such as cell seeding, transfection reagent or quantity of DNA transfected, are involved in GPCR expression in cell lines and should be explored to optimize functional expression in cell-based assays.

CRediT authorship contribution statement

Christine Belloir: Writing – review & editing, Writing – original draft, Visualization, Validation, Resources, Project administration, Methodology, Investigation, Funding acquisition, Formal analysis, Data curation, Conceptualization. **Adèle Gautier:** Visualization, Validation, Investigation. **Adeline Karolkowski:** Writing – review & editing, Visualization. **Thomas Delompré:** Visualization, Validation, Investigation. **Mathilde Jeannin:** Visualization, Investigation. **Lucie Moitrier:** Investigation. **Fabrice Neiers:** Writing – review & editing, Supervision. **Loïc Briand:** Writing – review & editing, Supervision, Project administration, Funding acquisition, Conceptualization.

Funding sources

Declaration of competing interest

The authors declare that they have no known competing financial interests or personal relationships that could have appeared to influence the work reported in this paper.

Acknowledgements

Appendix A. Supplementary data

Supplementary data to this article can be found online at https://doi.org/10.1016/j.pep.2024.106643.

Data availability

Data will be made available on request.

References

[1] L. Briand, C. Salles, Taste perception and integration, in: P. Etiévant, E. Guichard, C. Salles, A. Voilley (Eds.), Flavor from Food to Behaviors, Wellbeing and Health, Elsevier Ltd., Duxford, UK, 2016, pp. 101–119, https://doi.org/10.1016/B978-0-08-100295-7.00004-9.

[2] I. Nissim, A. Dagan-Wiener, M.Y. Niv, The taste of toxicity: a quantitative analysis of bitter and toxic molecules, IUBMB 69 (2017) 938–946, https://doi.org/10.1002/iub.1694.

[3] S.D. Roper, Taste buds as peripheral chemosensory processors, Semin. Cell Dev. Biol. 24 (2013) 71–79, https://doi.org/10.1016/j.semcdb.2012.12.002.

[4] E. Adler, M.A. Hoon, K.L. Mueller, J. Chandrashekar, N.J.P. Ryba, C.S. Zuker, A novel family of mammalian taste receptors, Cell 100 (2000) 693–702, https://doi.org/10.1016/S0092-8674(00)80705-9.

[5] J. Chandrashekar, K.L. Mueller, M.A. Hoon, E. Adler, L. Feng, W. Guo, C.S. Zuker, N.J.P. Ryba, T2Rs function as bitter taste receptors, Cell 100 (2000) 703–711, https://doi.org/10.1016/S0092-8674(00)80706-0.

[6] H. Matsunami, J.-P. Montmayeur, L.B. Buck, A family of candidate taste receptors in human and mouse, Nature 404 (2000) 601–604, https://doi.org/10.1038/35007072.

[7] J.-P. Montmayeur, S.D. Liberles, H. Matsunami, L.B. Buck, A candidate taste receptor gene near a sweet taste locus, Nat. Neurosci. 4 (2001) 492–498, https://doi.org/10.1038/87440.

[8] W. Meyerhof, C. Batram, C. Kuhn, A. Brockhoff, E. Chudoba, B. Bufe, G. Appendino, M. Behrens, The molecular receptive ranges of human TAS2R bitter taste receptors, Chem. Senses 35 (2010) 157–170, https://doi.org/10.1093/chemse/bjp092.

[9] E. Chamoun, N.A. Carroll, L.M. Duizer, W. Qi, Z. Feng, G. Darlington, A.M. Duncan, J. Haines, D.W.L. Ma, The guelph family health study, the relationship between single nucleotide polymorphisms in taste receptor genes, taste function and dietary intake in preschool-aged children and adults in the guelph family health study, Nutrients 10 (2018) 990, https://doi.org/10.3390/nu10080990.

[10] S.P. Pydi, R.P. Bhullar, P. Chelikani, Chapter ten - constitutive activity of bitter taste receptors (T2Rs), in: Y.-X. Tao (Ed.), Advances in Pharmacology, Academic Press, 2014, pp. 303–326, https://doi.org/10.1016/B978-0-12-417197-8.00010-9.

[11] D.R. Reed, T. Tanaka, A.H. McDaniel, Diverse tastes: genetics of sweet and bitter perception, Physiol. Behav. 88 (2006) 215–226, https://doi.org/10.1016/j.physbeh.2006.05.033.

[12] N. Roudnitzky, M. Behrens, A. Engel, S. Kohl, S. Thalmann, S. Hübner, K. Lossow, S.P. Wooding, W. Meyerhof, Receptor polymorphism and genomic structure interact to shape bitter taste perception, PLoS Genet. 11 (2015) e1005530, https://doi.org/10.1371/journal.pgen.1005530.

[13] T. Ueda, S. Ugawa, Y. Ishida, Y. Shibata, S. Murakami, S. Shimada, Identification of coding single-nucleotide polymorphisms in human taste receptor genes involving bitter tasting, Biochem. Biophys. Res. Commun. 285 (2001) 147–151, https://doi.org/10.1006/bbrc.2001.5136.

[14] A. Dagan-Wiener, A. Di Pizio, I. Nissim, M.S. Bahia, N. Dubovski, E. Margulis, M.Y. Niv, BitterDB: taste ligands and receptors database in 2019, Nucleic Acids Res. 47 (2019) D1179–D1185, https://doi.org/10.1093/nar/gky974.

[15] M. Behrens, A. Brockhoff, C. Kuhn, B. Bufe, M. Winnig, W. Meyerhof, The human taste receptor hTAS2R14 responds to a variety of different bitter compounds, Biochem. Biophys. Res. Commun. 319 (2004) 479–485, https://doi.org/10.1016/j.bbrc.2004.05.019.

[16] A. Levit, S. Nowak, M. Peters, A. Wiener, W. Meyerhof, M. Behrens, M.Y. Niv, The bitter pill: clinical drugs that activate the human bitter taste receptor TAS2R14, Faseb. J. 28 (2014) 1181–1197, https://doi.org/10.1096/fj.13-242594.

[17] S. Nowak, A. Di Pizio, A. Levit, M.Y. Niv, W. Meyerhof, M. Behrens, Reengineering the ligand sensitivity of the broadly tuned human bitter taste receptor TAS2R14, Biochim. Biophys. Acta Gen. Subj. 1862 (2018) 2162–2173, https://doi.org/10.1016/j.bbagen.2018.07.009.

[18] A. Karolkowski, C. Belloir, G. Lucchi, C. Martin, E. Bouzidi, L. Levavasseur, C. Salles, L. Briand, Activation of bitter taste receptors by saponins and alkaloids identified in faba beans (*Vicia faba* L. *minor*), Food Chem. 426 (2023) 136548, https://doi.org/10.1016/j.foodchem.2023.136548.

[19] Y. Kim, R.H. Gumpper, Y. Liu, D.D. Kocak, Y. Xiong, C. Cao, Z. Deng, B.E. Krumm, M.K. Jain, S. Zhang, J. Jin, B.L. Roth, Bitter taste receptor activation by cholesterol and an intracellular tastant, Nature 628 (2024) 664–671, https://doi.org/10.1038/s41586-024-07253-y.

[20] X. Hu, W. Ao, M. Gao, L. Wu, Y. Pei, S. Liu, Y. Wu, F. Zhao, Q. Sun, J. Liu, L. Jiang, X. Wang, Y. Li, Q. Tan, J. Cheng, F. Yang, C. Yang, J. Sun, T. Hua, Z.-J. Liu, Bitter taste TAS2R14 activation by intracellular tastants and cholesterol, Nature 631 (2024) 459–466, https://doi.org/10.1038/s41586-024-07569-9.

[21] L. Tao, D. Wang, Q. Yuan, F. Zhao, Y. Zhang, T. Du, S. Shen, H.E. Xu, Y. Li, D. Yang, J. Duan, Bitter taste receptor TAS2R14 activation and G protein assembly by an intracellular agonist, Cell Res. 34 (2024) 735–738, https://doi.org/10.1038/s41422-024-00995-4.

[22] M. Behrens, W. Meyerhof, Oral and extraoral bitter taste receptors, in: W. Meyerhof, U. Beisiegel, H.-G. Joost (Eds.), Sensory and Metabolic Control of Energy Balance, Springer, Berlin, Heidelberg, 2010, pp. 87–99, https://doi.org/10.1007/978-3-642-14426-4_8.

[23] M. Behrens, W. Meyerhof, Gustatory and extragustatory functions of mammalian taste receptors, Physiol. Behav. 105 (2011) 4–13, https://doi.org/10.1016/j.physbeh.2011.02.010.

[24] P. Lu, C.-H. Zhang, L.M. Lifshitz, R. ZhuGe, Extraoral bitter taste receptors in health and disease, JGP 149 (2017) 181–197, https://doi.org/10.1085/jgp.201611637.

[25] F.A. Shaik, N. Singh, M. Arakawa, K. Duan, R.P. Bhullar, P. Chelikani, Bitter taste receptors: extraoral roles in pathophysiology, Int. J. Biochem. Cell Biol. 77 (2016) 197–204, https://doi.org/10.1016/j.biocel.2016.03.011.

[26] D. Campa, P. Vodicka, B. Pardini, A. Naccarati, M. Carrai, L. Vodickova, J. Novotny, K. Hemminki, A. Försti, R. Barale, F. Canzian, A gene-wide investigation on polymorphisms in the taste receptor 2R14 (TAS2R14) and susceptibility to colorectal cancer, BMC Med. Genet. 11 (2010) 88, https://doi.org/10.1186/1471-2350-11-88.

[27] M.C. Chen, S.V. Wu, J.R. Reeve, E. Rozengurt, Bitter stimuli induce Ca2+ signaling and CCK release in enteroendocrine STC-1 cells: role of L-type voltage-sensitive Ca2+ channels, Am. J. Physiol. Cell Physiol. 291 (2006) C726–C739, https://doi.org/10.1152/ajpcell.00003.2006.

[28] C.D. Dotson, L. Zhang, H. Xu, Y.-K. Shin, S. Vigues, S.H. Ott, A.E.T. Elson, H.J. Choi, H. Shaw, J.M. Egan, B.D. Mitchell, X. Li, N.I. Steinle, S.D. Munger, Bitter taste receptors influence glucose homeostasis, PLoS One 3 (2008) e3974, https://doi.org/10.1371/journal.pone.0003974.

[29] M.M. Gaida, C. Mayer, U. Dapunt, S. Stegmaier, P. Schirmacher, G.H. Wabnitz, G.M. Hänsch, Expression of the bitter receptor T2R38 in pancreatic cancer: localization in lipid droplets and activation by a bacteria-derived quorum-sensing molecule, Oncotarget 7 (2016) 12623–12632, https://doi.org/10.18632/oncotarget.7206.

[30] H.-J. Jang, Z. Kokrashvili, M.J. Theodorakis, O.D. Carlson, B.-J. Kim, J. Zhou, H. H. Kim, X. Xu, S.L. Chan, M. Juhaszova, M. Bernier, B. Mosinger, R.F. Margolskee, J.M. Egan, Gut-expressed gustducin and taste receptors regulate secretion of glucagon-like peptide-1, Proc. Natl. Acad. Sci. U. S. A. 104 (2007) 15069–15074, https://doi.org/10.1073/pnas.0706890104.

[31] I. Kaji, S. Karaki, Y. Fukami, M. Terasaki, A. Kuwahara, Secretory effects of a luminal bitter tastant and expressions of bitter taste receptors, T2Rs, in the human and rat large intestine, J Physiol Gastrointest Liver Physiol 296 (2009) G971–G981, https://doi.org/10.1152/ajpgi.90514.2008.

[32] D.A. Deshpande, W.C.H. Wang, E.L. McIlmoyle, K.S. Robinett, R.M. Schillinger, S. S. An, J.S.K. Sham, S.B. Liggett, Bitter taste receptors on airway smooth muscle bronchodilate by localized calcium signaling and reverse obstruction, Nat. Med. 16 (2010) 1299–1304, https://doi.org/10.1038/nm.2237.

[33] T.E. Finger, B. Böttger, A. Hansen, K.T. Anderson, H. Alimohammadi, W.L. Silver, Solitary chemoreceptor cells in the nasal cavity serve as sentinels of respiration, Proc. Natl. Acad. Sci. U. S. A. 100 (2003) 8981–8986, https://doi.org/10.1073/pnas.1531172100.

[34] B.M. Hariri, D.B. McMahon, B. Chen, J.R. Freund, C.J. Mansfield, L.J. Doghramji, N.D. Adappa, J.N. Palmer, D.W. Kennedy, D.R. Reed, P. Jiang, R.J. Lee, Flavones modulate respiratory epithelial innate immunity: anti-inflammatory effects and activation of the T2R14 receptor, J. Biol. Chem. 292 (2017) 8484–8497, https://doi.org/10.1074/jbc.M116.771949.

[35] S.C. Kinnamon, Taste receptor signalling – from tongues to lungs, Acta Physiol. 204 (2012) 158–168, https://doi.org/10.1111/j.1748-1716.2011.02308.x.

[36] R.J. Lee, N.A. Cohen, Taste receptors in innate immunity, Cell. Mol. Life Sci. 72 (2015) 217–236, https://doi.org/10.1007/s00018-014-1736-7.

[37] R.J. Lee, G. Xiong, J.M. Kofonow, B. Chen, A. Lysenko, P. Jiang, V. Abraham, L. Doghramji, N.D. Adappa, J.N. Palmer, D.W. Kennedy, G.K. Beauchamp, P.-T. Doulias, H. Ischiropoulos, J.L. Kreindler, D.R. Reed, N.A. Cohen, T2R38 taste receptor polymorphisms underlie susceptibility to upper respiratory infection, J. Clin. Invest. 122 (2012) 4145–4159, https://doi.org/10.1172/JCI64240.

[38] A.S. Shah, Y. Ben-Shahar, T.O. Moninger, J.N. Kline, M.J. Welsh, Motile cilia of human airway epithelia are chemosensory, Science 325 (2009) 1131–1134, https://doi.org/10.1126/science.1173869.

[39] M. Tizzano, B.D. Gulbransen, A. Vandenbeuch, T.R. Clapp, J.P. Herman, H. M. Sibhatu, M.E.A. Churchill, W.L. Silver, S.C. Kinnamon, T.E. Finger, Nasal chemosensory cells use bitter taste signaling to detect irritants and bacterial signals, Proc. Natl. Acad. Sci. U. S. A. 107 (2010) 3210–3215, https://doi.org/10.1073/pnas.0911934107.

[40] S.R. Foster, E.R. Porrello, B. Purdue, H.-W. Chan, A. Voigt, S. Frenzel, R.D. Hannan, K.M. Moritz, D.G. Simmons, P. Molenaar, E. Roura, U. Boehm, W. Meyerhof, W. G. Thomas, Expression, regulation and putative nutrient-sensing function of taste GPCRs in the heart, PLoS One 8 (2013) e64579, https://doi.org/10.1371/journal.pone.0064579.

[41] F. Li, Taste perception: from the tongue to the testis, Mol. Hum. Reprod. 19 (2013) 349–360, https://doi.org/10.1093/molehr/gat009.

[42] L.T.P. Martin, M.W. Nachtigal, T. Selman, E. Nguyen, J. Salsman, G. Dellaire, D. J. Dupré, Bitter taste receptors are expressed in human epithelial ovarian and prostate cancers cells and noscapine stimulation impacts cell survival, Mol. Cell. Biochem. 454 (2019) 203–214, https://doi.org/10.1007/s11010-018-3464-z.

[43] K. Zheng, P. Lu, E. Delpapa, K. Bellve, R. Deng, J.C. Condon, K. Fogarty, L. M. Lifshitz, T.A.M. Simas, F. Shi, R. ZhuGe, Bitter taste receptors as targets for tocolytics in preterm labor therapy, Faseb. J. 31 (2017) 4037–4052, https://doi.org/10.1096/fj.201601323RR.

[44] N. Singh, R. Chakraborty, R.P. Bhullar, P. Chelikani, Differential expression of bitter taste receptors in non-cancerous breast epithelial and breast cancer cells, Biochem. Biophys. Res. Commun. 446 (2014) 499–503, https://doi.org/10.1016/j.bbrc.2014.02.140.

[45] T.C. Lund, A.J. Kobs, A. Kramer, M. Nyquist, M.T. Kuroki, J. Osborn, D.S. Lidke, S. T. Low-Nam, B.R. Blazar, J. Tolar, Bone marrow stromal and vascular smooth muscle cells have chemosensory capacity via bitter taste receptor expression, PLoS One 8 (2013) e58945, https://doi.org/10.1371/journal.pone.0058945.

[46] E. Reszka, E. Nowakowska-Świrta, M. Kupczyk, W. Dudek, D. Świerczyńska-Machura, T. Wittczak, J. Rykała, P. Monika, E. Jabłońska, B. Kręcisz, P. Kuna, W. Wąsowicz, C. Pałczyński, Expression of bitter taste receptors in the human skin, J. Clin. Res. Bioeth. 6 (2015), https://doi.org/10.4172/2155-9627.1000218.

[47] L. Shaw, C. Mansfield, L. Colquitt, C. Lin, J. Ferreira, J. Emmetsberger, D.R. Reed, Personalized expression of bitter 'taste' receptors in human skin, PLoS One 13 (2018) e0205322, https://doi.org/10.1371/journal.pone.0205322.

[48] B. Ansoleaga, P. Garcia-Esparcia, R. Pinacho, J.M. Haro, B. Ramos, I. Ferrer, Decrease in olfactory and taste receptor expression in the dorsolateral prefrontal cortex in chronic schizophrenia, J. Psychiatr. Res. 60 (2015) 109–116, https://doi.org/10.1016/j.jpsychires.2014.09.012.

[49] D. Herrera Moro Chao, C. Argmann, M. Van Eijk, R.G. Boot, R. Ottenhoff, C. Van Roomen, E. Foppen, J.E. Siljee, U.A. Unmehopa, A. Kalsbeek, J.M.F.G. Aerts, Impact of obesity on taste receptor expression in extra-oral tissues: emphasis on hypothalamus and brainstem, Sci. Rep. 6 (2016) 29094, https://doi.org/10.1038/srep29094.

[50] S. Janssen, J. Laermans, P.-J. Verhulst, T. Thijs, J. Tack, I. Depoortere, Bitter taste receptors and α-gustducin regulate the secretion of ghrelin with functional effects on food intake and gastric emptying, Proc. Natl. Acad. Sci. U. S. A. 108 (2011) 2094–2099, https://doi.org/10.1073/pnas.1011508108.

[51] N. Singh, M. Vrontakis, F. Parkinson, P. Chelikani, Functional bitter taste receptors are expressed in brain cells, Biochem. Biophys. Res. Commun. 406 (2011) 146–151, https://doi.org/10.1016/j.bbrc.2011.02.016.

[52] A.A. Clark, C.D. Dotson, A.E.T. Elson, A. Voigt, U. Boehm, W. Meyerhof, N. I. Steinle, S.D. Munger, TAS2R bitter taste receptors regulate thyroid function, Faseb. J. 29 (2015) 164–172, https://doi.org/10.1096/fj.14-262246.

[53] A. Di Pizio, L.A.W. Waterloo, R. Brox, S. Löber, D. Weikert, M. Behrens, P. Gmeiner, M.Y. Niv, Rational design of agonists for bitter taste receptor TAS2R14: from modeling to bench and back, Cell. Mol. Life Sci. 77 (2020) 531–542, https://doi.org/10.1007/s00018-019-03194-2.

[54] B. Bufe, T. Hofmann, D. Krautwurst, J.-D. Raguse, W. Meyerhof, The human TAS2R16 receptor mediates bitter taste in response to β-glucopyranosides, Nat. Genet. 32 (2002) 397–401, https://doi.org/10.1038/ng1014.

[55] M. Raliou, M. Grauso, B. Hoffmann, C. Schlegel–Le-Poupon, C. Nespoulous, H. Débat, C. Belloir, A. Wiencis, M. Sigoillot, S. Preet Bano, D. Trotier, J.-C. Pernollet, J.-P. Montmayeur, A. Faurion, L. Briand, Human genetic polymorphisms in T1R1 and T1R3 taste receptor subunits affect their function, Chem. Senses 36 (2011) 527–537, https://doi.org/10.1093/chemse/bjr014.

[56] I. Stein, A. Itin, P. Einat, R. Skaliter, Z. Grossman, E. Keshet, Translation of vascular endothelial growth factor mRNA by internal ribosome entry: implications for translation under hypoxia, Mol. Cell Biol. 18 (1998) 3112–3119, https://doi.org/10.1128/MCB.18.6.3112.

[57] C. Ammon, J. Schäfer, O.J. Kreuzer, W. Meyerhof, Presence of a plasma membrane targeting sequence in the amino-terminal region of the rat somatostatin receptor 3, Arch. Physiol. Biochem. 110 (2002) 137–145, https://doi.org/10.1076/apab.110.1.137.908.

[58] D. Krautwurst, K.-W. Yau, R.R. Reed, Identification of ligands for olfactory receptors by functional expression of a receptor library, Cell 95 (1998) 917–926, https://doi.org/10.1016/S0092-8674(00)81716-X.

[59] S.E. Jacobsen, U. Gether, H. Bräuner-Osborne, Investigating the molecular mechanism of positive and negative allosteric modulators in the calcium-sensing receptor dimer, Sci. Rep. 7 (2017) 46355, https://doi.org/10.1038/srep46355.

[60] P. Wellendorph, N. Burhenne, B. Christiansen, B. Walter, H. Schmale, H. Bräuner-Osborne, The rat GPRC6A: cloning and characterization, Gene 396 (2007) 257–267, https://doi.org/10.1016/j.gene.2007.03.008.

[61] T.P. Hopp, K.S. Prickett, V.L. Price, R.T. Libby, C.J. March, D. Pat Cerretti, D. L. Urdal, P.J. Conlon, A short polypeptide marker sequence useful for recombinant protein identification and purification, Nat. Biotechnol. 6 (1988) 1204–1210, https://doi.org/10.1038/nbt1088-1204.

[62] T. Ueda, S. Ugawa, H. Yamamura, Y. Imaizumi, S. Shimada, Functional interaction between T2R taste receptors and G-protein α subunits expressed in taste receptor cells, J. Neurosci. 23 (2003) 7376–7380, https://doi.org/10.1523/JNEUROSCI.23-19-07376.2003.

[63] Y. Zhang, X. Wang, X. Li, S. Peng, S. Wang, C.Z. Huang, C.Z. Huang, Q. Zhang, D. Li, J. Jiang, Q. Ouyang, Y. Zhang, S. Li, Y. Qiao, Identification of a specific agonist of human TAS2R14 from Radix Bupleuri through virtual screening, functional evaluation and binding studies, Sci. Rep. 7 (2017) 12174, https://doi.org/10.1038/s41598-017-11720-0.

[64] A. Einhauer, A. Jungbauer, Affinity of the monoclonal antibody M1 directed against the FLAG peptide, J Chromatograph A 921, 25–30, https://doi.org/10.1016/S0021-9673(01)00831-7, 2001.

[65] A. Einhauer, A. Jungbauer, The FLAG^{TM} peptide, a versatile fusion tag for the purification of recombinant proteins, J. Biochem. Biophys. Methods 49 (2001) 455–465, https://doi.org/10.1016/S0165-022X(01)00213-5.

[66] W.S.U. Roland, R.J. Vincken, R.J. Gouka, L. van Buren, H. Gruppen, G. Smit, Soy isoflavones and other isoflavonoids activate the human bitter taste receptors hTAS2R14 and hTAS2R39, J. Agric. Food Chem. 59 (2011) 11764–11771, https://doi.org/10.1021/jf202816u.

[67] H. Xu, L. Staszewski, H. Tang, E. Adler, M. Zoller, X. Li, Different functional roles of T1R subunits in the heteromeric taste receptors, Proc. Natl. Acad. Sci. USA 101 (2004) 14258–14263, https://doi.org/10.1073/pnas.0404384101.

[68] C. Belloir, M. Brulé, L. Tornier, F. Neiers, L. Briand, Biophysical and functional characterization of the human TAS1R2 sweet taste receptor overexpressed in a HEK293S inducible cell line, Sci. Rep. 11 (2021) 22238, https://doi.org/10.1038/s41598-021-01731-3.

[69] C. Belloir, M. Jeannin, A. Karolkowski, C. Scott, L. Briand, A receptor-based assay to study the sweet and bitter tastes of sweeteners and binary sweet blends: the SWEET Project, Chem. Senses (2024), https://doi.org/10.1093/chemse/bjae041 bjae041.

[70] C. Tower-Gilchrist, M.L. Styers, B.K. Yoder, N.F. Berbari, E. Sztul, Chapter fifteen - monitoring endosomal trafficking of the G protein-coupled receptor somatostatin receptor 3, in: P.M. Conn (Ed.), Methods in Enzymology, Academic Press, 2014, pp. 261–280, https://doi.org/10.1016/B978-0-12-397926-1.00015-9.

[71] S.A. War, R.K. Somvanshi, U. Kumar, Somatostatin receptor-3 mediated intracellular signaling and apoptosis is regulated by its cytoplasmic terminal, Biochim. Biophys. Acta 1813 (2011) 390–402, https://doi.org/10.1016/j.bbamcr.2010.12.015.

[72] C.G. Tate, R. Grisshammer, Heterologous expression of G-protein-coupled receptors, Trends Biotechnol. 14 (1996) 426–430, https://doi.org/10.1016/0167-7799(96)10059-7.

[73] H. Zhuang, H. Matsunami, Evaluating cell-surface expression and measuring activation of mammalian odorant receptors in heterologous cells, Nat. Protoc. 3 (2008) 1402–1413, https://doi.org/10.1038/nprot.2008.120.

[74] B.D. Shepard, N. Natarajan, R.J. Protzko, O.W. Acres, J.L. Pluznick, A cleavable N-terminal signal peptide promotes widespread olfactory receptor surface expression in HEK293T cells, PLoS One 8 (2013) e68758, https://doi.org/10.1371/journal.pone.0068758.

[75] R. Emter, C. Merillat, S. Dossenbach, A. Natsch, The trilogy of human musk receptors: linking receptor activation, genotype, and sensory perception, Chem. Senses 49 (2024) bjae015, https://doi.org/10.1093/chemse/bjae015.

[76] R. Emter, C. Mérillat, F. Buchli, A. Natsch, Expression of Odorant Receptors Reveals Unique Specificity of Human Sense of Smell for Signature Odorants, 2024.

[77] K. Palczewski, T. Kumasaka, T. Hori, C.A. Behnke, H. Motoshima, B.A. Fox, I. L. Trong, D.C. Teller, T. Okada, R.E. Stenkamp, M. Yamamoto, M. Miyano, Crystal structure of rhodopsin: a G protein-coupled receptor, Science 289 (2000) 739–745, https://doi.org/10.1126/science.289.5480.739.

[78] S. Chaudhary, J.E. Pak, B.P. Pedersen, L.J. Bang, L.B. Zhang, S.M.M. Ngaw, R. G. Green, V. Sharma, R.M. Stroud, Efficient expression screening of human membrane proteins in transiently transfected Human Embryonic Kidney 293S cells, Methods 55 (2011) 273–280, https://doi.org/10.1016/j.ymeth.2011.08.018.

[79] A. Malhotra, Chapter 16 tagging for protein expression, in: R.R. Burgess, M. P. Deutscher (Eds.), Methods in Enzymology, Academic Press, 2009, pp. 239–258, https://doi.org/10.1016/S0076-6879(09)63016-0.

[80] S.T. Loughran, D. Walls, Tagging recombinant proteins to enhance solubility and aid purification, in: D. Walls, S.T. Loughran (Eds.), Protein Chromatography: Methods and Protocols, Springer, New York, NY, 2017, pp. 131–156, https://doi.org/10.1007/978-1-4939-6412-3_8.

[81] D.S. Waugh, Making the most of affinity tags, Trends Biotechnol. 23 (2005) 316–320, https://doi.org/10.1016/j.tibtech.2005.03.012.

[82] P.M. Schmidt, L.G. Sparrow, R.M. Attwood, X. Xiao, T.E. Adams, J.L. McKimm-Breschkin, Taking down the FLAG! How insect cell expression challenges an established tag-system, PLoS One 7 (2012) e37779, https://doi.org/10.1371/journal.pone.0037779.

[83] M. Sandal, M. Behrens, A. Brockhoff, F. Musiani, A. Giorgetti, P. Carloni, W. Meyerhof, Evidence for a transient additional ligand binding site in the TAS2R46 bitter taste receptor, J. Chem. Theor. Comput. 11 (2015) 4439–4449, https://doi.org/10.1021/acs.jctc.5b00472.

[84] C. Bushdid, C.A. de March, J. Topin, M. Do, H. Matsunami, J. Golebiowski, Mammalian class I odorant receptors exhibit a conserved vestibular-binding pocket, Cell. Mol. Life Sci. 76 (2019) 995–1004, https://doi.org/10.1007/s00018-018-2996-4.

[85] J. Upadhyaya, N. Singh, R.P. Bhullar, P. Chelikani, The structure–function role of C-terminus in human bitter taste receptor T2R4 signaling, Biochim. Biophys. Acta 1848 (2015) 1502–1508, https://doi.org/10.1016/j.bbamem.2015.03.035.

[86] S.P. Pydi, A. Jaggupilli, K.M. Nelson, S.R. Abrams, R.P. Bhullar, M.C. Loewen, P. Chelikani, Abscisic acid acts as a blocker of the bitter taste G protein-coupled receptor T2R4, Biochemistry 54 (2015) 2622–2631, https://doi.org/10.1021/acs.biochem.5b00265.

[87] S.G.F. Rasmussen, B.T. DeVree, Y. Zou, A.C. Kruse, K.Y. Chung, T.S. Kobilka, F. S. Thian, P.S. Chae, E. Pardon, D. Calinski, J.M. Mathiesen, S.T.A. Shah, J.A. Lyons, M. Caffrey, S.H. Gellman, J. Steyaert, G. Skiniotis, W.I. Weis, R.K. Sunahara, B. K. Kobilka, Crystal structure of the β2 adrenergic receptor–Gs protein complex, Nature 477 (2011) 549–555, https://doi.org/10.1038/nature10361.

[88] T.M. Gupte, R.U. Malik, R.F. Sommese, M. Ritt, S. Sivaramakrishnan, Priming GPCR signaling through the synergistic effect of two G proteins, Proc. Natl. Acad. Sci. U. S. A. 114 (2017) 3756–3761, https://doi.org/10.1073/pnas.1617232114.

[89] M. Behrens, J. Bartelt, C. Reichling, M. Winnig, C. Kuhn, W. Meyerhof, Members of RTP and REEP gene families influence functional bitter taste receptor expression, J. Biol. Chem. 281 (2006) 20650–20659, https://doi.org/10.1074/jbc.M513637200.

[90] H. Saito, M. Kubota, R.W. Roberts, Q. Chi, H. Matsunami, RTP family members induce functional expression of mammalian odorant receptors, Cell 119 (2004) 679–691, https://doi.org/10.1016/j.cell.2004.11.021.

[91] L. Wu, Y. Pan, G.-Q. Chen, H. Matsunami, H. Zhuang, Receptor-transporting protein 1 short (RTP1S) mediates translocation and activation of odorant receptors by acting through multiple steps, J. Biol. Chem. 287 (2012) 22287–22294, https://doi.org/10.1074/jbc.M112.345884.

[92] H. Zhuang, H. Matsunami, Synergism of accessory factors in functional expression of mammalian odorant receptors, J. Biol. Chem. 282 (2007) 15284–15293, https://doi.org/10.1074/jbc.M700386200.

[93] K. Yoshikawa, K. Touhara, Myr-Ric-8A enhances G(alpha15)-mediated Ca2+ response of vertebrate olfactory receptors, Chem. Senses 34 (2009) 15–23, https://doi.org/10.1093/chemse/bjn047.

[94] L.E.C. Von Dannecker, A.F. Mercadante, B. Malnic, Ric-8B, an olfactory putative GTP exchange factor, amplifies signal transduction through the olfactory-specific G-protein gαolf, J. Neurosci. 25 (2005) 3793–3800, https://doi.org/10.1523/JNEUROSCI.4595-04.2005.

[95] L.E.C. Von Dannecker, A.F. Mercadante, B. Malnic, Ric-8B promotes functional expression of odorant receptors, Proc. Natl. Acad. Sci. U. S. A. 103 (2006) 9310–9314, https://doi.org/10.1073/pnas.0600697103.

[96] E. Ilegems, K. Iwatsuki, Z. Kokrashvili, O. Benard, Y. Ninomiya, R.F. Margolskee, REEP2 enhances sweet receptor function by recruitment to lipid rafts, J. Neurosci. 30 (2010) 13774–13783, https://doi.org/10.1523/JNEUROSCI.0091-10.2010.

[97] C. Reichling, W. Meyerhof, M. Behrens, Functions of human bitter taste receptors depend on N-glycosylation, J. Neurochem. 106 (2008) 1138–1148, https://doi.org/10.1111/j.1471-4159.2008.05453.x.